Use of Sn–Si nanocomposite electrodes for Li rechargeable batteries

Hyo-Jin Ahn, Youn-Su Kim, Kyung-Won Park and Tae-Yeon Seong*

Received (in Cambridge, UK) 13th May 2004, Accepted 1st November 2004
First published as an Advance Article on the web 23rd November 2004
DOI: 10.1039/b407264b

The relationship between the structural properties of Sn nano-dots embedded in a Si electrode synthesised by co-sputtering and their electrochemical performance during a lithium insertion and extraction process has been investigated.

Due to the reduction in size of electronic device features, there is a constant demand for lithium rechargeable batteries which have greater battery capacity. In order to improve the performance of Li rechargeable batteries, the development of new anodic materials which have capacities greater than that of carbon (372 mA h g^{-1}) is required.[1] Silicon has been considered as a promising anode because of its high capacity (theoretical capacity, 980 μA h (cm^2 × μm)$^{-1}$), compared with currently used carbon or graphite.[2–4] Despite this high capacity, however, a pure Si electrode suffers from poor cyclability due to mechanical cracking caused by the volume change occurring during the insertion and extraction processes.[5,6] For the enhancement of performance, such as reversible capacity, modification of the electrode structure seems to be a vital factor.[7] Recently, the introduction of nano-sized materials in battery systems has been suggested to be a possibility since the physical, electrical and chemical properties of nanophases are very different from those of their bulk counterparts.[8–11] It is believed that the key to the successful application of nanostructured electrodes in batteries is a combination of a number of reaction sites, a fast transport pathway for electrons and ions, and the cycle performance of the battery.[9,10,12] Indeed, the use of nano-sized electrodes was shown to strongly affect the reversible capacity of batteries.[13] For example, Wang *et al.*[14] reported that nano-sized NiSi and FeSi powders prepared by high-energy ball-milling yield a high Li storage capacity. Recently, Song *et al.*,[15] while investigating the film thickness dependence of the electrochemical behaviour of nanocrystalline Mg_2Si thin film electrodes, showed that the nano-sized structure of the anodes is important for improving the electrochemical performance of Li rechargeable batteries. Li and Martin,[16] while investigating the electrochemical behaviour of SnO_2 particles embedded within the anode of Li rechargeable batteries, suggested that the nano-sized Sn grains in the SnO_2 nanofibers result in improved cycling performance. In this work, we have investigated the synthesis and electrochemical properties of a two-phase nanocomposite electrode, *i.e.*, Sn nano-dots embedded in a Si electrode prepared by a co-sputtering system. It is shown that the addition of Sn nano-dots effectively improves the cycling performance of Li rechargeable batteries.

Sn–Si nanocomposite electrodes were deposited on Cu foil substrates using an RF magnetron sputtering system, at a base pressure of less than 5×10^{-6} Torr and a working pressure of 5×10^{-3} Torr. Sputtering was carried out under an inert Ar gas atmosphere at 40 sccm at room temperature. Three different nanocomposite electrodes (1 × 1 cm in area) were synthesised: sample A (230 nm thick) was deposited for 30 min at RF powers of 30 W (Si target) and 30 W (Sn target); sample B (236 nm) for 25 min at RF powers of 60 W (Si target) and 30 W (Sn target), and sample C (244 nm) for 20 min at RF powers of 90 W (Si target) and 30 W (Sn target). For comparison, a Si single-phase electrode was also prepared at 50 W for 30 min. The thicknesses of the nanocomposite electrodes were carefully measured using field emission scanning electron microscopy (FESEM: Hitachi S-4100). To measure the thickness accurately, the electrodes were intentionally deposited onto Pt/Si substrates instead of Cu substrates, since the Pt/Si substrates were easy to cut into pieces for measurements. The microstructures of the nanocomposite electrodes were examined using high-resolution electron microscopy (HREM) (a Phillips CM20T/STEM electron microscope at 200 kV). X-Ray diffraction (XRD) examinations were done using a Rigaku X-ray diffractometer equipped with a Cu Kα source. X-ray photoelectron spectroscopy (XPS) analyses were carried out using a VG Scientific (ESCALAB 250) X-ray photoelectron spectrometer with an Al Kα X-ray source (1486.6 eV) at a base pressure of 2×10^{-9} Torr. To evaluate the electrochemical performance of the nanocomposite electrodes, the electrochemical behaviour for Li insertion and extraction was investigated using a conventional two-electrochemical system. Test cells fabricated with as-deposited thin-film working electrodes and metallic Li anodes were prepared in a glove box filled with Ar gas. A 1.0 M $LiPF_6$ solution in a 1 : 1 (vol%) mixture of ethylene carbonate and diethyl carbonate was used as the electrolyte. The test cells were aged for 12 h at 25 °C after the addition of the electrolyte before electrochemical testing. The electrochemical behaviour of the nanocomposite electrodes was investigated in organic electrolyte Li cells using a WBCS 3000 battery tester system (Won-A Tech Corp., Korea) with a constant current density of 20 μA cm^{-2} at a cut-off voltage of 0.1 to 2.0 V (*vs.* Li/Li^+) at room temperature.

Fig. 1 shows HREM images and transmission electron diffraction (TED) patterns obtained from the pure Si thin-film and Sn–Si nanocomposite electrodes. For the Si electrode (Fig. 1(a)), the image reveals uniform speckle contrast and the TED pattern exhibits a broad diffuse ring, which are characteristics of amorphous materials. For the nanocomposite samples, the HREM images exhibit a number of dark blobs. A comparison of the Si and Sn–Si nanocomposite samples indicates that the blobs are Sn nano-dots and are embedded in an amorphous Si electrode (bright contrast). The TED patterns also revealed a characteristic of amorphous phases, indicating that the Sn nano-dots have amorphous structure. This was further confirmed by XRD results (not shown), which showed the presence of a very weak broad diffraction peak, a characteristic of amorphous structure. The Sn

*tyseong@gist.ac.kr

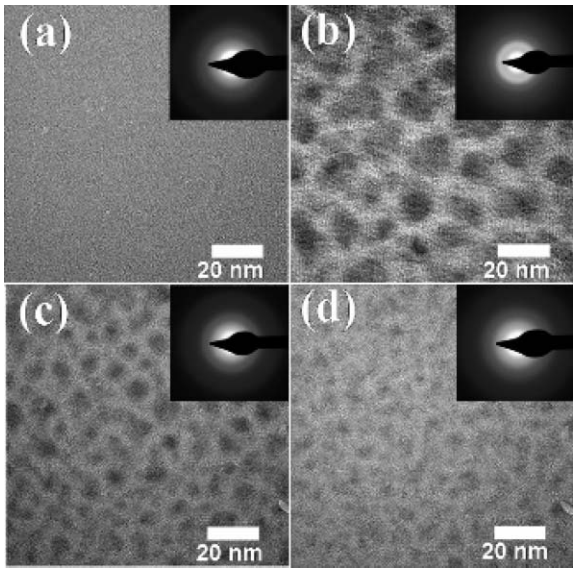

Fig. 1 HREM images of (a) a pure Si electrode fabricated by conventional sputtering and (b) Si–Sn nanocomposite sample A, (c) sample B, and (d) sample C that were fabricated by a co-sputtering method. Their transmission electron diffraction (TED) patterns are shown in the inset (top right).

nano-dots are measured to be in the range 8–19, 4–9, and 4–6.5 nm for samples A, B, and C respectively.

XPS analyses were made of the three nanocomposite samples. A charge correction was applied to the C 1s (284.5 eV) signal, and all other XPS peaks in the C 1s, Si 2p and Sn 3d regions. The Sn $3d_{5/2}$ XPS spectrum exhibited a signal corresponding to the Sn metallic state (~485.0 eV).[17] This is in good agreement with the thermodynamic solubility of Sn in Si;[18] due to its low solubility, the incorporated Sn tends to be segregated in the amorphous matrix. Furthermore, the Si 2p spectrum appears at ~99.0 eV.[17] It was shown that the relative intensities of the Sn spectral peaks decrease with increasing RF power for the Si target. This indicates that a larger amount of Sn was incorporated into the Si electrode when the samples were synthesised at lower RF power for the Si target, as summarised in Table 1. In addition, the Sn 3d XPS results show that tin oxide is present in the form of SnO_2 at the surface region of the Sn nano-dots. The XPS results also show that the oxidation states of Si 2p is Si^{4+} (~103.3 eV)[17] and that silicon oxide forms only at the surface during exposure to air for the XPS examination.

Fig. 2 shows the cycle number dependence of the insertion capacities of Li/Sn–Si cells fabricated with the three different Sn–Si

Table 1 Summary of the amounts of Sn and Si in the three different Si–Sn nanocomposite electrodes, which were calculated by $C_x = (I_x/S_x)/(\Sigma i_i/S_i)$ based on the XPS spectra

		Sensitivity factor (S_x)	Area (I_x)	Atom fraction of constituent (C_x)
Sample A	Sn 3d	4.095	106 469.12	Sn : Si = 0.67 : 0.33
	Si 2p	0.283	3644.90	
Sample B	Sn 3d	4.095	86 208.18	Sn : Si = 0.49 : 0.51
	Si 2p	0.283	6341.25	
Sample C	Sn 3d	4.095	47 478.73	Sn : Si = 0.24 : 0.76
	Si 2p	0.283	8640.72	

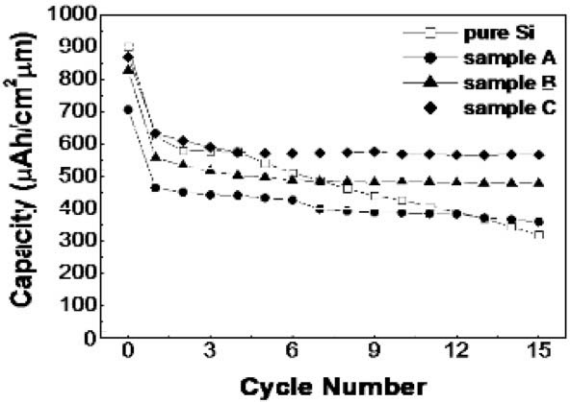

Fig. 2 The cycle number dependence of the capacities of Li/Sn–Si cells fabricated with the three different Sn–Si nanocomposite electrodes, in which the cut-off voltages were 0.1 to 2.0 V.

nanocomposite electrodes. It is shown that the cycling performance of the pure Si thin film-based cells rapidly degrades with increasing cycle number.[7] However, the Sn–Si nanocomposite electrode-based cells exhibit good stability. In other words, as the cycle number increases, the capacity drops by 27–33% of the initial value and then becomes saturated. This indicates that although the amorphous Si plays a major role in producing high capacity, the presence of the Sn nano-dots delays the degradation of the capacity by stabilizing the amorphous Si matrix, and so is very effective in enhancing the electrochemical performance of batteries. This is in good agreement with the results previously reported by other groups, showing that the incorporation of nanostructured electrodes into batteries enhances the electrochemical performance of Li ion batteries.[9–12,19] Although the exact mechanism for the Sn nano-dot dependence of the cycling behaviour is not clear at this moment, the improvement of the cycling behaviour of the Sn–Si nanocomposite-based cells can be attributed to the increased structural stability of the electrodes, namely, a decrease in the volume change of the Si electrode due to the incorporation of the Sn nano-dots.[9] In other words, the Si electrode-based cells suffered a large loss in the capacity due to the mechanical cracking caused by the volume change during the cycling process.[5,6] It is also noted that the capacity performance is dependent on the amount of Sn (and its size) incorporated in the amorphous Si electrode, namely, the smaller the size of the Sn nano-dots, the better the capacity. For example, the cells made with the samples A, B, and C produced capacities of 707.0, 829.0, and 870.0 μA h $(cm^2 \times \mu m)^{-1}$ in the first insertion process, respectively. Considering that Sn has a lower theoretical capacity than Si,[20] the reason why sample C yields a higher capacity than samples A and B can be associated with the smaller amount of Sn nano-dots incorporated in the Si electrode. The capacity drops by 49.1, 42.2, and 34.8% of the initial value after 15 cycles for samples A, B, and C, respectively, showing that sample C gives higher capacity than samples A and B. This indicates that smaller Sn nano-dots are more effective in minimising the volume expansion and hence hindering the cracking of the Si electrode film, leading to better capacity performance.

Fig. 3 shows insertion curves for the samples with the three different Sn–Si nanocomposite electrodes, in which the cut-off voltages were 0.1 to 2.0 V. It is shown that capacity depends on the amount of incorporated Sn.

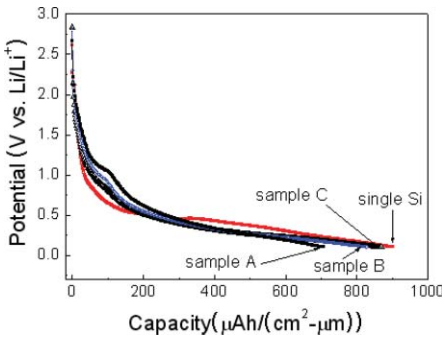

Fig. 3 Potential *vs.* capacity curves for Li/Sn–Si cells made with three different Sn–Si nanocomposite electrodes with a constant current density of 20 μA cm^{-2} at a cut-off voltage of 0.1 to 2.0 V.

In summary, the nanocomposite electrodes, *i.e.*, Sn nano-dots embedded in the amorphous Si electrode, were designed and synthesised using a co-sputtering system. Li/Sn–Si cells fabricated with the Sn–Si nanocomposite electrodes showed very good reversible capacity during the Li insertion and extraction process, which is much better than that of the cells with the pure Si film electrodes. This implies that the use of the Sn–Si nanocomposite electrodes is potentially important for realising high-performance Li rechargeable batteries.

Hyo-Jin Ahn, Youn-Su Kim, Kyung-Won Park and Tae-Yeon Seong*
Department of Materials & Science Engineering, Gwangju Institute of Science & Technology (GIST), Gwangju 500-712, Republic of Korea. E-mail: tyseong@gist.ac.kr; Fax: +82 62 970 2304; Tel: +82 62 970 2308

Notes and references

1 J.-M. Tarascon and M. Armand, *Nature*, 2001, **414**, 359.
2 M. Winter, J. O. Besenhard, M. E. Spahr and P. Novak, *Adv. Mater.*, 1998, **10**, 725.
3 H. Li, X. Huang, L. Chen, G. Zhou, Z. Zhang, D. Yu, Y. J. Mo and N. Pei, *Solid State Ionics*, 2000, **135**, 181.
4 C. Wang, A. J. Appleby and F. E. Little, *J. Power Sources*, 2001, **93**, 174.
5 J. O. Basenhard, P. Komenda, A. Paxinos, E. Wudy and M. Josowicz, *Solid State Ionics*, 1986, **18**, 823.
6 J. O. Basenhard, M. Hess and P. Komenda, *Solid State Ionics*, 1990, **40**, 525.
7 S. Bourderau, T. Brousse and D. M. Schleich, *J. Power Sources*, 1999, **81**, 233.
8 H.-J. Ahn, H.-C. Choi, K.-W. Park, S.-B. Kim and Y.-E. Sung, *J. Phys .Chem. B*, 2004, **108**, 9815.
9 H.-J. Ahn, K.-W. Park and Y.-E. Sung, *Chem. Mater.*, 2004, **16**, 1991.
10 G. S. Attard, J. M. Elliott, P. N. Bartlett, A. Whitehead and J. R. Owen, *Macromol. Symp.*, 2000, **156**, 179.
11 P. Poizot, S. Laruelle, S. Grugeon, L. Dupont and J.-M. Tarascon, *Nature*, 2000, **407**, 496.
12 N. Li, C. R. Martin and B. Scrosati, *J. Power Sources*, 2001, **97**, 240.
13 J. O. Basenhard, J. Yang and M. Winter, *J. Power Sources*, 1997, **68**, 87.
14 G. X. Wang, L. Sun, D. H. Bradhurst, S. Zhong, S. X. Dou and H. K. Liu, *J. Power Sources*, 2000, **88**, 278.
15 S.-W. Song, K. A. Striebel, R. P. Reade, G. A. Roberts and E. J. Cairns, *J. Electrochem. Soc.*, 2003, **150**, 121.
16 N. Li and C. R. Martin, *J. Electrochem. Soc.*, 2001, **148**, 164.
17 J. F. Moulder, W. F. Stickle, P. E. Sobol and K. D. Bomben, *Handbook of X-ray Photoelectron Spectroscopy*, Physical Electronics, Eden Prairie, MN, 1995.
18 T. B. Massalski, H. Okamoto, P. R. Subramanian and L. Kacprzak, *Binary Alloy Phase Diagrams*, ASM International, Materials Park, OH, 2nd edn., 1990, **vol. 3**, p. 3361.
19 D. Aurbach, A. Nimberger, B. Markovsky, E. Levi, E. Sominski and A. Gedanken, *Chem. Mater.*, 2002, **14**, 4155.
20 J. Wang, I. D. Raistrick and R. A. Huggins, *J. Electrochem. Soc.*, 1986, **133**, 457.